Asian Journal of Chemistry; Vol. 38, No. 6 (2026), 1652-1662
ASIAN JOURNAL OF CHEMISTRY
https://doi.org/10.14233/ajchem.2026.35929

Computational Design, Synthesis and Biological Evaluation of Some Novel 1*H*-Pyrrolizine Carboxylic Acid Derivatives as Anticancer Agents

SUBHASH CHANDER[1,2], KARAN GOEL[1], KATARZYNA WANKE[3,4], MATEUSZ KCIUK[3], RENATA KONTEK[3], THAKUR GURJEET SINGH[1] and SOMDUTT MUJWAR[1,*]

[1]Chitkara College of Pharmacy, Chitkara University, Rajpura-140401, India
[2]Research and Development Department, Valence Lab, Jansui Village, Rajpura-140401, India
[3]Department of Molecular Biotechnology and Genetics, University of Lodz, 90-237 Lodz, Poland
[4]Doctoral School of Exact and Natural Sciences, University of Lodz, Banacha Street 12/16, 90-237 Lodz, Poland

*Corresponding author: E-mail: somduttmujwar@gmail.com

Received: 10 March 2026 *Accepted*: 25 May 2026 *Published online*: 31 May 2026 AJC-22392

Licofelone is a 1*H*-pyrrolizine carboxylic acid based dual COX/5-LOX inhibitor, emerges as a promising therapeutic candidate due to its ability to simultaneous interference of both inflammatory pathways, but its clinical translation is restricted by its poor pharmacokinetics. The current research aims to design novel 1*H*-pyrrolizine carboxylic acid derivatives with the intent to improve the pharmacokinetics and explore their anticancer potential. The docking analysis of the designed analogues showed potent binding with COX-2, 5-LOX and some other anticancer targets, especially indoleamine 2,3-dioxygenase-1 (IDO1), in comparison with parent molecule. A synthetic procedure was developed and optimised for the synthesis of designed compounds followed by assessing their anticancer potential by performing an MTT assay. The obtained results have concluded that the designed licofelone-derived pyrrolizine analogues revealed that structural modifications with different amino acid conjugates significantly influenced their anticancer activity with compound **8b** and **8c** exhibited the most potent antiproliferative activity against PANC-1 cells with IC_{50} values of 1.7 ± 0.2 μM and 1.4 ± 0.05 μM, respectively. These molecules can be further used to develop novel anticancer therapeutics post preclinical and clinical validation.

Keywords: Licofelone, Anticancer activity, Docking studies, MTT assay, COX/5-LOX inhibitor, 1*H*-Pyrrolizine carboxylic acid.

INTRODUCTION

Licofelone is a pyrrolizine based heterocyclic agent reported for its anti-inflammatory effects. Chemically it is 2,2-dimethyl-6-(4-chlorophenyl)-7-phenyl-2,3-dihydro-1*H*-pyrrolizine-5-yl acetic acid. Structurally, it contains a pyrolizine core substituted with 4-chlorophenyl and phenyl rings, along with an acetic acid side chain [1]. The unique structural arrangement of licofelone enables it as a dual inhibitor of cyclooxygenase-2 (COX-2) and 5-lipoxygenase (5-LOX) for exerting anti-inflammatory effect distinguishing it from conventional NSAIDs [2]. The presence of aromatic hydrophobic groups facilitates favourable interactions within enzyme active sites, while the carboxylic acid moiety contributes to target binding through hydrogen-bonding and ionic interactions. These structural features have made licofelone an attractive scaffold for the design of novel anti-inflammatory and anticancer agents [3].

From a medicinal chemistry perspective, licofelone has a highly functionalised heterocyclic framework with a bicyclic pyrrolizine nucleus fused to multiple aromatic substituent groups, which collectively contribute to its pharmacological profile [4-6]. The central pyrrolizine ring system consists of a nitrogen-containing 5-membered ring fused with a partially aromatic carbocyclic system, providing structural rigidity and an ideal electronic distribution for interaction with receptors. The presence of the *para*-chlorophenyl group at the 6-position significantly improves the lipophilic character of the molecule and increases the contact area with the active sites of the COX-2 and 5-LOX enzymes [7-10]. Further modulation of the electron density of the aromatic ring by the electron withdrawing chlorine makes the compound more metabolically stable and enhances its binding affinity. Moreover, the phenyl group at the 7-position contributes to π–π stacking interactions with hydrophobic amino acid residues located in the enzyme-binding pocket, providing further selectivity and

inhibitory potency. The 2,2-dimethyl substitution on the pyrolizine ring may enhance the molecule's conformational stability and steric bulk, potentially affecting receptor selectivity and metabolic stability. Another chemically significant feature of licofelone is the presence of an acetic acid functionality attached to the pyrrolizine framework [7,8]. This acidic functional group plays an important role in biological activity allowing the formation of ionic and hydrogen-bonding interactions with amino acid residues within the catalytic domains of inflammatory enzymes. The carboxylic acid group also contributes to the compound's partial hydrophilicity, influencing its solubility, absorption and pharmacokinetic profile. In addition, the pyrrolizine nucleus contains a nitrogen atom that can serve as a hydrogen-bond acceptor, thereby stabilising ligand–receptor interactions and increasing biological activity. Although licofelone demonstrates strong anti-inflammatory effects, its clinical application is hindered by poor pharmacokinetics including low bioavailability and metabolic instability [7-11]. As a result, extensive medicinal chemistry studies have focused on structural modifications of the licofelone scaffold to target novel 1*H*-pyrrolizine carboxylic acid derivatives with enhanced pharmacological and pharmacokinetic properties.

Non-steroidal anti-inflammatory drugs (NSAIDs) have attracted considerable interest for their anticancer effect due to their potential to suppress the inflammatory reactions associated with the progression of cancer *via* targeting the root cause for the same [12]. Licofelone is an established anti-inflammatory agent with a distinctive mode of action *via* dual interference of COX and LOX pathways, impacting angiogenesis, cell proliferation and apoptosis processes related to the progression of cancer. Some of the recent studies have concluded that the dual inhibitory effect of licofelone makes it more effective than conventional NSAIDs targeting only COX enzymes [7,9]. Thus, an attempt has been made to design and synthesize licofelone-amino acid conjugates with optimised pharmacokinetic for improved therapeutic effects. The designed lead molecules were then tested for their anticancer potential by MTT assays to highlight the critical role of the pyrrolizine pharmacophore in the design of novel anticancer agents with enhanced-potency, selectivity and biological safety.

EXPERIMENTAL

All solvents and reagents used for synthesis were of analytical reagent (AR) grade and procured from commercial suppliers. Amino acids, hydrazine hydrate, oxalyl chloride, thionyl chloride, triethylamine, EDC·HCl and HOBt were used without further purification. Reaction progress was monitored by thin-layer chromatography (TLC) using silica gel plates and visualised under UV light. Purification of synthesised compounds was performed by column chromatography using silica gel (60-120 mesh). Structural characterisation was carried out using nuclear magnetic resonance (^{1}H & ^{13}C NMR) Bruker instrument Avance spectrometer and mass spectrometry (LCMS/MS): AB SCIEX, USA (model: 4000QTRAP).

General synthesis of licofelone: Synthesis of licofelone analogues involves multistep series of reactions. Same reported reaction conditions with partial modification, if required, will be adapted to get significant yield and quality of licofelone analogues. 5-Benzyl-3,3-dimethyl-3,4-dihydro-2*H*-pyrrole (**1**) reacts with 2-2-bromo-1-(4-chlorophenyl)ethan-1-one to prepare licofelone intermediate. Licofelone intermediate further reacts with oxalyl chloride and hydrazine hydrate to form licofelone (**Scheme-I**).

Step-1: Synthesis of 6-(4-chlorophenyl)-2.2-dimethyl-7-phenyl-2.3-dihydro-l-*H*-pyrrolizine (3): 5-Benzyl-3,3-dimethyl-3,4-dihydro-2*H*-pyrrole (**1**) (50.0 g, 0.266 mol) was dissolved in methanol (500 mL) in a suitably sized reaction vessel and the resulting solution was cooled to 15-20 ºC. To this solution, 2-bromo-4′-chloroacetophenone (**2**) (65.45 g, 0.280 mol) was added portion-wise over 15-30 min with continuous stirring. Sodium bicarbonate (44.85 g, 0.534 mol) was then added and the reaction mixture was stirred at 20-25 ºC for 24 h under exclusion of light. Upon completion of the reaction, as indicated by the formation of a yellowish suspension, the solid product was isolated by suction filtration and washed with cold methanol. The wet solid was suction-dried and subsequently suspended in water, followed by stirring at 40-45 ºC for 30-35 min to remove inorganic impurities. The resulting solid was collected by suction filtration and dried under reduced pressure at 35-40 ºC to afford 6-(4-chlorophenyl)-2.2-dimethyl-7-phenyl-2.3-dihydro-l-*H*-pyrrolizine (**3**) (yield: 51.55 g, 60.0 %).

Step-2: Synthesis of 6-(4-chlorophenyl)-2.2-dimethyl-7-phenyl-2.3-dihydro-l-*H*-pyrrolizin-5-yl-acetic acid (6): 6-(4-Chlorophenyl)-2,2-dimethyl-7-phenyl-2,3-dihydro-1*H*-pyrrolizine (**3**) (50.0 g, 0.155 mol) was dissolved in anhydrous THF (300 mL) under stirring and the reaction vessel was purged and maintained under a nitrogen atmosphere. The resulting yellow solution was cooled to 10-15 ºC and oxalyl chloride (31.6 g, 0.248 mol) was added dropwise over 10-15 min, ensuring that the internal temperature remained below 15 ºC. Upon completion of the addition, the reaction mixture, which developed a green colouration, was stirred at 18-25 ºC for an additional 20-30 min. The reaction was cautiously quenched by the controlled addition in crushed ice (80 g), maintaining the internal temperature below 20 ºC, followed by stirring at 20-30 ºC for 5-10 min. 2-methoxy ethanol (270 g) and hydrazine hydrate (60.0 g, 1.872 mol) were then added and the temperature was gradually increased while THF was distilled off until the reaction temperature reached 75-80 ºC. The resulting suspension was cooled to 50-55 ºC and KOH (113.0 g, 2.02 mol) was added portion-wise over 30 min.

The reaction mixture was then heated gradually to 95-110 ºC, during which significant frothing was observed; this was controlled by increased stirring and continuous N_2 gas sparging through a dip tube. The temperature was further raised slowly to 140-145 ºC and aqueous distillate was collected. The reaction mixture was maintained at 130-145 ºC for 2-3 h before cooling to 35-40 ºC. Subsequently, water and diethyl ether were added and the biphasic mixture was stirred vigorously for 15-20 min. After phase separation, the aqueous layer was isolated, cooled to below 5 ºC and acidified to pH 1 with aqueous HCl, keeping the temperature below 10 ºC. The resulting precipitate was extracted with diethyl ether and the combined organic extracts were washed thoroughly with water and treated with activated charcoal. The solvent was

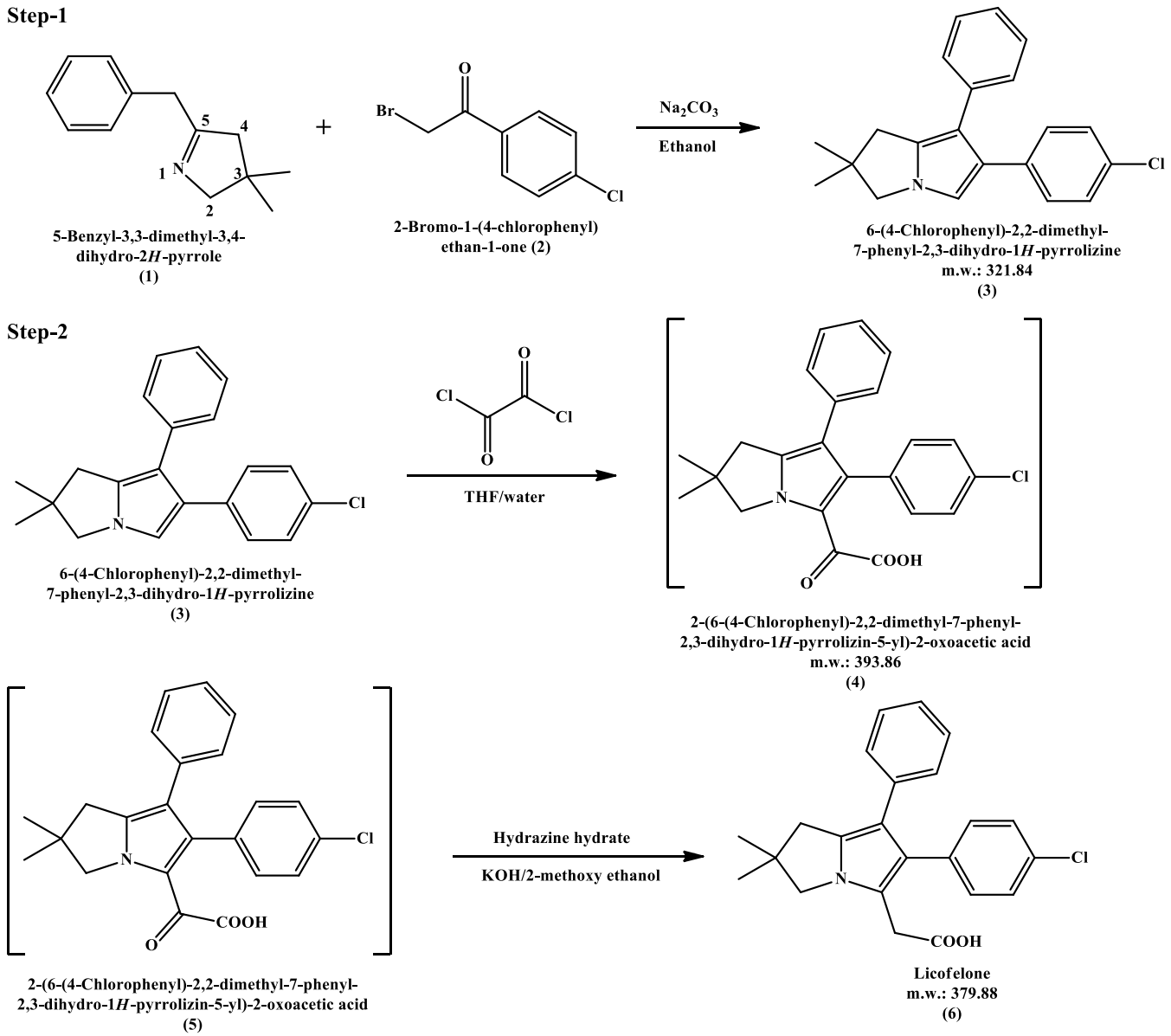

Scheme-I: Synthesis route for 2-(6-(4-chlorophenyly)-2,2-dimethyl-7-phenyl-2,3-dihydro-1*H*-pyrolizin-5-yl)acetic acid

removed under reduced pressure below 20 ºC. The resulting solid was slurred in heptane, collected by suction filtration, washed with heptane and dried under vacuum at 45-55 ºC to afford 6-(4-chlorophenyl)-2.2-dimethyl-7-phenyl-2.3-dihydro-l-*H*-pyrrolizin-5-yl-acetic acid (**6**) (yield: 27.21 g, 46.0%).

Synthesis of 1*H*-pyrrolizine carboxylic acid-amino acid conjugates: Based on an analogue design supported by molecular modelling studies, a 1*H*-pyrrolizine carboxylic acid derivative was designed and synthesised. The molecular modelling results guided the structural modification of licofelone and the target compound was prepared according to the reaction scheme described in **Scheme-II** [13,14].

Step-3: Synthesis of 1*H*-pyrrolizine carboxylic acid-amino acid conjugates (8a-h): Amino acids **7a-h** (1.00 equiv.) were suspended in anhydrous dichloromethane (10.0 mL) in a round-bottom flask under a N_2 atmosphere. The reaction mixture was cooled to 10-15 ºC and thionyl chloride (1.10 equiv.) was added dropwise over 10-15 min while maintaining the internal temperature below 15 ºC. After complete addition, the mixture was heated at reflux for 3-4 h. Reaction progress was monitored by TLC. The reaction was quenched by the slow addition of methanol (20.0 mL), followed by stirring at 25-30 ºC for 45-60 min. The solvent was removed under reduced pressure and the residue was dissolved in aqueous $NaHCO_3$ (10%) and extracted with ethyl acetate (3 × 25 mL). The combined organic layers were concentrated and used directly in the next step without further purification. Licofelone **6** (0.95 equiv) was dissolved in anhydrous CH_2Cl_2 (10.0 mL) under nitrogen and cooled to 0-5 ºC. Triethylamine (2.00 equiv.) was added dropwise over 10-15 min, followed by EDC·HCl (1.20 equiv) and HOBt (1.20 equiv.), while maintaining the temperature below 5 ºC. The reaction mixture was stirred at 25-30 ºC for 3-4 h, with TLC monitoring. Upon completion, water (20 mL) was added and the mixture was stirred for 10 min. The layers were separated and the aqueous phase was extracted with dichloromethane (2 × 20 mL). The

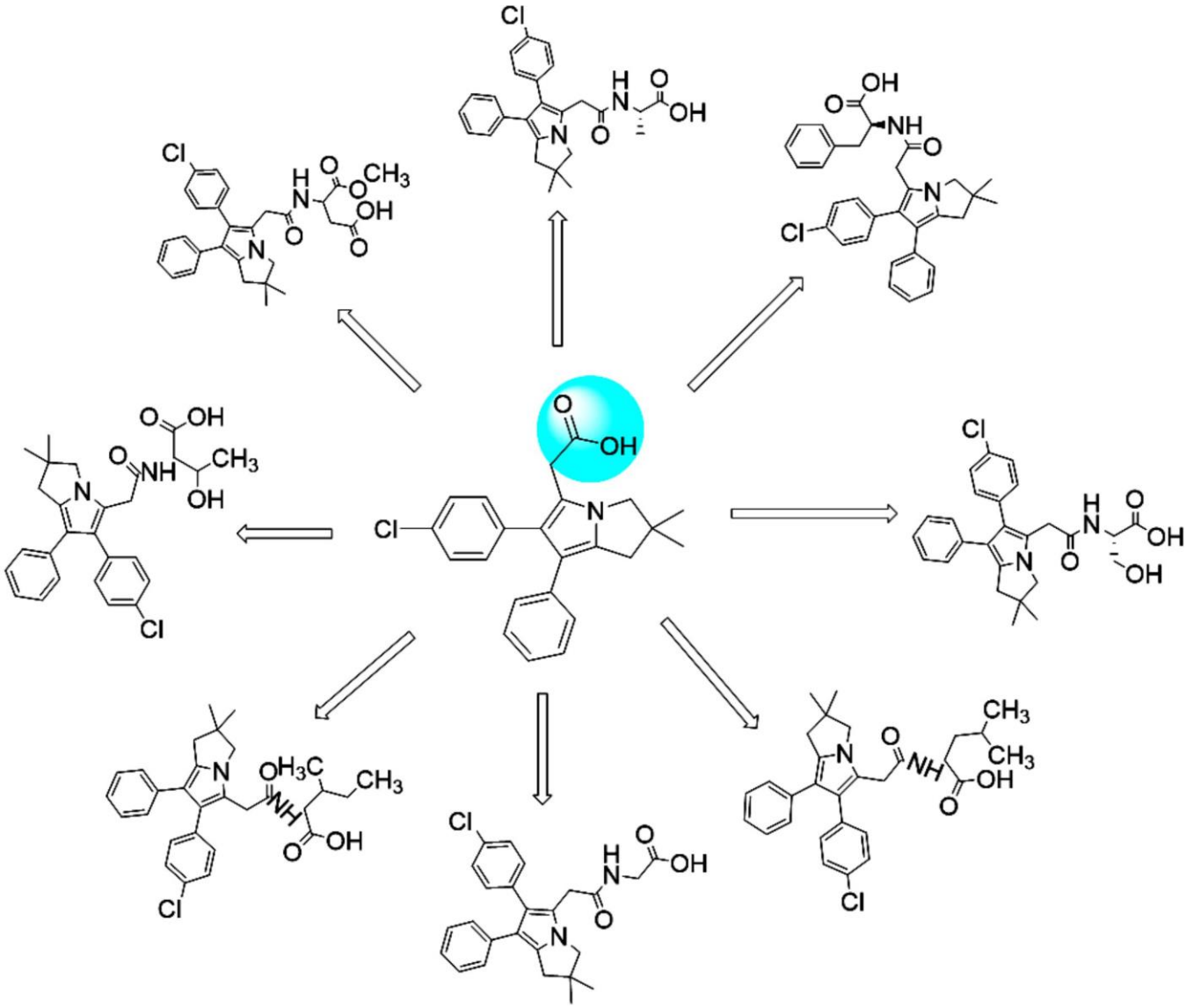

Scheme-II: Analogue designing of licofelone

combined organic extracts were concentrated under reduced pressure to afford the crude product. The crude material was dissolved in MeOH/H_2O (2: 1, v/v) and cooled to 0-5 ºC. Sodium hydroxide (1.50 equiv.) was added portion-wise and the reaction mixture was stirred at 25-30 ºC for 3-4 h. After completion, solvents were removed under reduced pressure, the residue was diluted with water and extracted with CH_2Cl_2 (3 × 20 mL). The aqueous layer was adjusted to pH 7 using 1.0 N HCl and extracted with CH_2Cl_2 (3 × 20 mL). The combined organic layers were washed with water, treated with activated charcoal and concentrated under reduced pressure below 20 ºC (**Scheme-III**). The resulting solid was triturated with diethyl ether, collected by filtration, washed with diethyl ether and dried under vacuum at 45-55 ºC to afford the desired 1*H*-pyrrolizine carboxylic acid-amino acid conjugates **8a-h**.

(2-(6-(4-Chlorophenyl)-2,2-dimethyl-7-phenyl-2,3-dihydro-1*H*-pyrrolizin-5-yl)acetyl)alanine (8a): Pale yellow colour, yield: 62.0%; Anal. calcd. (found) %: C, 69.25 (69.11); H, 6.04 (6.02); N, 6.21 (6.19); ^{1}H NMR (125 MHz, DMSO-d_6, δ ppm): 1.21 (s, 6H), 1.70 (d, 3H), 2.78 (s, 2H), 3.48 (s, 2H), 3.73 (s, 2H), 4.39 (m, 1H), 6.99-7.03 (m, 3H), 7.12-7.15 (m, 4H), 7.28-7.30 (d, *J* = 8.35 Hz, 2H), 12.57 (s, 1H); ^{13}C NMR (500 MHz, DMSO-d_6, δ ppm): 15.50, 27.47, 31.00, 40.08, 42.72, 51.25, 57.72, 113.76, 118.88, 121.99, 124.45, 127.70, 128.03, 128.11, 130.42, 131.41, 133.48, 135.06, 135.94, 171.96, 175.40; MS (ESI): calculated for $C_{26}H_{27}ClN_2O_3$ *m/z* 450.96, found $[M+H]^+$ *m/z* 451.8.

((2-(6-(4-Chlorophenyl)-2,2-dimethyl-7-phenyl-2,3-dihydro-1*H*-pyrrolizin-5-yl)acetyl)glutamic acid) (8b): Yellow colour Yield: 60.0%; Anal. calcd. (found) %: C, 66.07 (65.94); H, 5.74 (5.73); N, 5.50 (5.49); ^{1}H NMR (125 MHz, DMSO-d_6, δ ppm): 1.21 (s, 6H), 2.05 (m, 2H), 2.70 (t, 2H), 2.78 (s, 2H), 3.48 (s, 2H), 3.73 (s, 2H), 4.55 (t, 1H), 6.99-7.03 (m, 3H), 7.12-7.15 (m, 4H), 7.28-7.30 (d, *J* = 8.35 Hz, 2H), 12.57 (s, 2H); ^{13}C NMR (500 MHz, DMSO-d_6, δ ppm): 26.01, 27.99, 30.42, 31.62, 32.54, 42.64, 58.10, 59.04, 113.76, 118.88, 121.99, 124.45, 127.70, 128.03, 128.11, 130.42, 131.41, 133.48, 135.06, 135.94, 171.62, 174.73, 175.15; MS

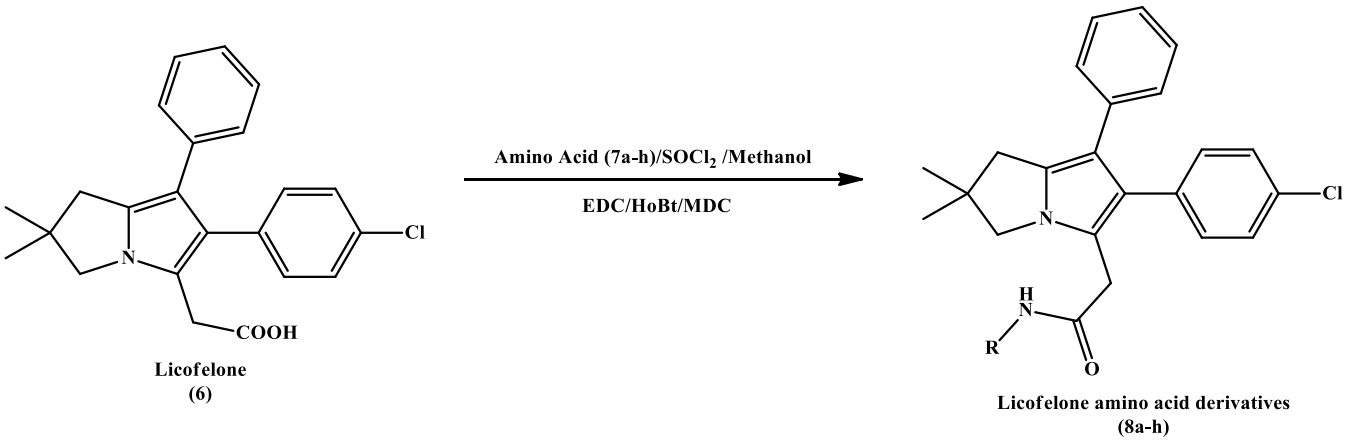

Scheme-III: Synthesis route for the 1*H*-pyrrolizine carboxylic acid-amino acids conjugates

(ESI): calculated for $C_{28}H_{29}ClN_2O_5$ *m/z* 508.99, found $[M+H]^+$ *m/z* 510.9.

(2-(6-(4-Chlorophenyl)-2,2-dimethyl-7-phenyl-2,3-dihydro-1*H*-pyrrolizin-5-yl)acetyl)proline) (8c): Yellow colour, yield: 64.0%; Anal. calcd. (found) %: C, 70.50 (70.36); H, 6.13 (6.11); N, 5.87 (5.86); ^{1}H NMR (125 MHz, DMSO-d_6, δ ppm): 1.21 (s, 6H), 1.75 (s, 2H), 1.92- 2.05 (t, 2H), 2.08-2.33 (m, 2H), 3.48 (s, 2H), 3.73 (s, 2H), 3.41-3.51 (t, 2H), 4.33 (s, 1H), 6.99-7.03 (m, 3H), 7.12-7.15 (m, 4H), 7.28-7.30 (d, *J* = 8.35 Hz, 2H), 12.57 (s, 1H); ^{13}C NMR (500 MHz, DMSO-d_6, δ ppm); 24.5, 26.93, 27.43, 31.10, 40.04, 42.60, 45.09, 56.60, 57.71, 112.98, 118.85, 121.48, 123.45, 127.50, 128.63, 128.91, 130.36, 131.45, 133.58, 135.54, 136.04, 171.48, 174.20; MS (ESI): calculated for $C_{28}H_{29}ClN_2O_3$ *m/z* 477.00, found $[M+H]^+$ *m/z* 478.8.

(2-(6-(4-Chlorophenyl)-2,2-dimethyl-7-phenyl-2,3-dihydro-1*H*-pyrrolizin-5-yl)acetyl)serine) (8d): Light yellow colour, yield: 62.0%; Anal. calcd. (found) % C, 66.88 (66.74); H, 5.82 (5.81); N, 5.99 (5.98); ^{1}H NMR (125 MHz, DMSO-d_6, δ ppm): 1.21 (s, 6H), 1.75 (s, 2H), 3.48 (s, 2H), 3.73 (s, 2H), 3.89-4.14 (m, 2H), 4.06 (t, 1H), 4.94 (s, 1H), 6.99-7.03 (m, 3H), 7.12-7.15 (m, 4H), 7.28-7.30 (d, *J* = 8.35 Hz, 2H), 8.32 (s, 1H), 12.39 (s, 2H); ^{13}C NMR (500 MHz, DMSO-d_6, δ ppm): 27.47, 31.00, 40.08, 42.72, 49.60, 50.72, 57.72, 113.76, 118.88, 121.99, 124.45, 127.70, 128.03, 128.11, 130.42, 131.41, 133.48, 135.06, 135.94, 170.40, 175.41; MS (ESI): calculated for $C_{26}H_{27}ClN_2O_4$ *m/z* 466.16, found $[M+H]^+$ *m/z* 468.7.

((2-(6-(4-Chlorophenyl)-2,2-dimethyl-7-phenyl-2,3-dihydro-1*H*-pyrrolizin-5-yl)acetyl)tryptophan) (8e): Pale yellow colour, yield: 61.5%; Anal. calcd. (found) %: C, 72.14 (71.99); H, 5.69 (5.68); N, 7.42 (7.40); ^{1}H NMR (125 MHz, DMSO-d_6, δ ppm): 1.21 (s, 6H), 1.75 (s, 2H), 3.06-3.31 (t, 2H), 3.48 (s, 2H), 3.73 (s, 2H), 4.72 (t, 1H), 6.99-7.03 (m, 5H), 7.12-7.15 (m, 4H), 7.20 (s, 1H), 7.28-7.30 (d, *J* = 8.35 Hz, 2H), 7.33-7.58 (m, 2H), 8.32 (s, 1H), 10.79 (s, 1H), 12.89 (s, 1H); ^{13}C NMR (500 MHz, DMSO-d_6, δ ppm): 26.23, 28.41, 31.25, 40.06, 42.62, 60.31, 61.41, 109.71, 111.10, 113.76, 118.84, 119.80, 121.76, 124.45, 127.70, 128.03, 128.11, 130.42, 131.41, 133.48, 135.06, 135.94, 136.05, 172.10, 174.36; MS (ESI): calculated for $C_{34}H_{32}ClN_3O_3$ *m/z*: 566.09, found $[M+H]^+$ *m/z*: 567.4.

((2-(6-(4-Chlorophenyl)-2,2-dimethyl-7-phenyl-2,3-dihydro-1*H*-pyrrolizin-5-yl)acetyl)glycine) (8f): Yellow colour, yield: 60.0%; Anal. calcd. (found) %: C, 68.72 (68.58); H, 5.76 (5.75); N, 6.41 (6.39); ^{1}H NMR (125 MHz, DMSO-d_6, δ ppm): 1.21 (s, 6H), 1.75 (s, 2H), 3.48 (s, 2H), 3.73 (s, 2H), 4.09 (s, 2H), 6.99-7.03 (m, 3H), 7.12-7.15 (m, 4H), 7.28-7.30 (d, *J* = 8.35 Hz, 2H), 9.03 (s, 1H), 12.39 (s, 1H); ^{13}C NMR (500 MHz, DMSO-d_6, δ ppm); 27.47, 31.00, 40.08, 41.07, 42.72, 57.72, 113.76, 118.88, 121.99, 124.45, 127.70, 128.03, 128.11, 130.42, 131.41, 133.48, 135.06, 135.94, 170.56, 175.32; MS (ESI): calculated for $C_{25}H_{25}ClN_2O_3$ *m/z*: 436.93, found $[M+H]^+$ *m/z*: 437.7.

(2-(6-(4-Chlorophenyl)-2,2-dimethyl-7-phenyl-2,3-dihydro-1*H*-pyrrolizin-5-yl)acetyl)aspartic acid (8g): Yellow colour, yield: 64.0%; Anal. calcd. (found) %: C, 65.52 (65.39); H, 5.49 (5.48); N, 5.66 (5.64); ^{1}H NMR (125 MHz, DMSO-d_6, δ ppm): 1.21 (s, 6H), 1.75 (s, 2H), 2.65-2.90 (d, 2H), 3.48 (s, 2H), 3.73 (s, 2H), 4.76 (t, 1H), 6.99-7.03 (m, 3H), 7.12-7.15 (m, 4H), 7.28-7.30 (d, *J* = 8.35 Hz 2H), 8.32 (s, 1H), 12.48 (s, 2H); ^{13}C NMR (500 MHz, DMSO-d_6, δ ppm); 28.10, 31.06, 35.90, 40.12, 42.78, 54.10, 57.72, 113.23, 118.28, 121.89, 123.95, 127.65, 128.32, 128.56, 130.85, 131.56, 133.38, 135.16, 136.01, 171.96, 174.56, 175.41; MS (ESI): calculated for $C_{27}H_{27}ClN_2O_5$ *m/z*: 494.97, found $[M+H]^+$ *m/z*: 496.5.

(2*R*)-5-Carbamimidamido-2-({[6-(4-chlorophenyl)-2,2-dimethyl-7-phenyl-2,3-dihydro-1*H*-pyrrolizin-5-yl]-acetyl}amino)pentanoic acid (8h): Light yellow colour, yield: 63.5%; Anal. calcd. (found) %: C, 64.97 (64.84); H, 6.39 (6.38); N, 13.06 (13.03); ^{1}H NMR (125 MHz, DMSO-d_6, δ ppm): 1.21 (s, 6H), 1.51 (m, 2H), 1.76 (m, 2H), 2.78 (s, 2H), 2.82 (s, 1H), 3.34 (m, 2H), 3.48 (s, 2H), 3.73 (s, 2H), 4.55 (s, 1H), 6.63 (s, 2H), 6.99-7.03 (m, 3H), 7.12-7.15 (m, 4H), 7.28-7.30 (d, *J* = 8.35 Hz 2H), 8.32 (s, 1H), 12.66 (s, 1H); ^{13}C NMR (500 MHz, DMSO-d_6, δ ppm); 24.60, 29.45, 29.78, 31.72, 32.63, 41.26, 42.70, 56.20, 57.70, 113.76, 118.88, 121.99, 124.45, 127.70, 128.03, 128.11, 130.42, 131.41, 133.48, 135.06, 135.94, 158.01, 171.63, 174.72; MS (ESI): calculated for $C_{29}H_{34}ClN_5O_3$ *m/z*: 536.07, found $[M+H]^+$ *m/z*: 537.6.

Biological evaluation

Cell culture: Human cancer cell lines (GSU, gastric carcinoma, RRID: CVCL_8877 and PANC-1, pancreatic carcinoma, CRL-1469™) were used for the biological evaluation of the synthesised 1*H*-pyrrolizine carboxylic acid derivatives. The GSU cell line was purchased from Creative Bioarray, Frankfurt am Main, while PANC-1 cells were obtained from the American Type Culture Collection, Rockville, MD, USA. GSU cells were cultured in RPMI-1640 medium and PANC-1 cells were maintained in Dulbecco's Modified Eagle's medium (DMEM). Both culture media were supplemented with 10% (v/v) fetal bovine serum (FBS) and 1% penicillin-streptomycin solution. The cells were maintained in a standard culture environment at 37 ºC in a humidified incubator with 5% (v/v) CO_2. The culture medium was refreshed every 24-48 h and upon reaching confluency, cells were passaged using 0.25% (w/v) trypsin-EDTA solution for further experimentation.

MTT assay: The *in vitro* cytotoxic activity of the newly synthesised 1*H*-pyrrolizine carboxylic acid derivatives (**8a-h**) was evaluated using the MTT assay. In brief, GSU and PANC-1 cancer cells were seeded in 96-well plates at a density of about 8 × 10^3 cells per 100 µL per well. Following an initial incubation period under standard culture conditions (37 ºC, 5% CO_2), the cells were incubated for 24 h with a series of dilutions of the synthesised derivatives **8a-h** in DMSO to obtain final concentrations ranging from 0.25 to 200 µM, in a total volume of 100 µL per well. The final DMSO concentration was maintained below 0.5% (v/v). Vehicle-treated controls and blank wells containing culture medium without cells were included in each experiment [15,16]. After 72 h incubation with the test compounds, 20 µL of MTT solution (5 mg/mL in PBS) was added to each well and further incubated for 3 h under identical conditions. After incubation, the supernatant was then carefully removed and 100 µL of DMSO was added to dissolve the formazan crystals formed by viable cells. The absorbance was measured at 570 nm using a PowerWave XS microplate reader (BioTek Instruments, Winooski, VT, USA). The experiments were conducted in duplicate and IC_{50} values were determined from dose-response curves by nonlinear regression [17,18].

Computational studies

Identification of the pharmacophores: The chemical structure of licofelone has been shortlisted as a potential pharmacophore and was investigated to identify the important pharmacophoric features and their role in chemical interactions with its reported molecular targets to identify potential substitution sites. Licofelone was selected as the parent pharmacophore for analogue development with the aim of improving its pharmacokinetic and pharmacodynamic properties because of its reported dual inhibitory potential against COX-2 and 5-LOX receptors [7,19-22]. Structural analysis revealed that the pyrrolizine scaffold and aryl-substituted moieties are crucial for hydrophobic and π-π interactions within the target binding pocket, whereas the terminal carboxylic acid moiety showed comparatively lower contribution to receptor binding and was therefore selected as the modification site. Based on this rationale, a focused ligand library of amino acid-conjugated 1*H*-pyrrolizine carboxylic acid derivatives was designed to enhance target affinity and drug-like properties while retaining the core pharmacophoric framework [21-23]. The ligands were sketched in ChemDraw 15 software and energy-minimised in Chem3D using the MM2 force field prior to molecular docking studies [24-27]. The basic chemical structure of licofelone used for analogue design is shown in Fig. 1. Based on this hypothesis, licofelone has been considered as a pharmacophore to develop its analogues with the intent to develop a novel molecule with improved pharmacokinetic and pharmacodynamic effects.

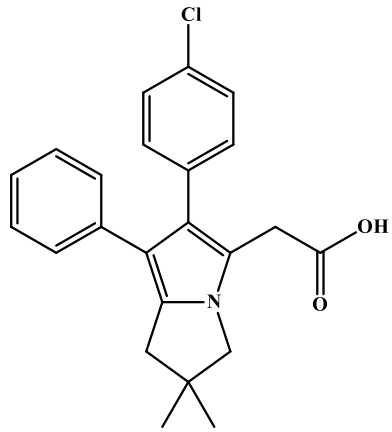

Fig. 1. Basic chemical structure of licofelone

Selection of anticancer targets: Diverse anticancer targets were explored based upon based on their established roles in inflammation-associated carcinogenesis, oxidative stress, immune evasion, *etc*. for execution of docking analysis of the designed licofelone-derived pyrrolizine analogues [28,29].

Molecular docking: The 3D crystal structures of the selected molecular targets, including COX-1 (PDB ID: 3KK6), COX-2 (PDB ID: 5IKR), LOX-2 (PDB ID: 3V99), 5-LOX (PDB ID: 6N2W), indoleamine 2,3-dioxygenase 1 (IDO1) (PDB ID: 9F5R) and retinoic acid receptor-related orphan receptor gamma (RORγ) (PDB ID: 6Q7A), were obtained from the RCSB Protein Data Bank [30,31]. The macromolecular target receptors were prepared for docking analysis by removing the co-crystallised ligands from the active site, then deleting redundant water molecules and adding polar hydrogen atoms. The reference ligands were separated, their rotatable and non-rotatable bonds were assigned before saving in the default *.pdbqt format required for docking simulations using AutoDock4.2 software [32,33]. The active ligand binding sites of the selected receptors were identified by analysing the interacting amino acid residues with their co-crystallised ligands using Discovery Studio 2021 software [34]. The identified active binding regions were used for defining the grid parameters and preparing the grid box for docking simulations. A 3D grid box was constructed to encompass the active pocket of the respective receptors. The AutoGrid implementation in the AutoDock suite was employed to generate atom-specific affinity maps for all ligand and receptor atom types. The Lamarckian Genetic Algorithm (LGA) was used as the main conformational search algorithm for molecular docking. Docking parameters were validated by re-docking the reference ligands into their active binding pockets and assessing

the docking scores, interaction profiles and the overlap between the docked poses and the crystallographically determined binding pose [35,36]. The designed 1*H*-pyrrolizine carboxylic acid analogues were subsequently docked into the active sites of all selected targets and the best docked conformations were selected based on minimum binding energy and favourable chemical interactions for further analysis [37-40].

Pharmacokinetic profiling: Pharmacokinetic profiling of the designed licofelone-derived pyrrolizine analogues was executed by using the pkCSM webserver to evaluate their absorption, distribution, metabolism, excretion, toxicity (ADMET) and drug-likeness properties. The chemical structures of the designed compounds were used to generate their SMILES to be provided as input in pkCSM webserver.

RESULTS AND DISCUSSION

A series of novel 1*H*-pyrrolizine carboxylic acid-amino acid conjugates (**8a-h**) were successfully designed and synthesized through a systematic multistep synthetic strategy starting from licofelone intermediates. The synthetic route efficiently incorporated structural modifications guided by molecular modelling studies, enabling the generation of diversified analogues with improved pharmacophoric features. The use of amino acid conjugation provided an opportunity to enhance the physico-chemical and pharmacokinetic properties of the parent licofelone scaffold. Furthermore, the introduction of amino acid moieties is expected to improve molecular interactions with biological targets through additional hydrogen-bonding and steric contributions.

Computational studies

Pharmacophore identification and ligand design: 1*H*-Pyrrolizine carboxylic acid has been identified as a pharmacophore to design its derivatives to develop new molecules with better pharmacokinetic and pharmacodynamic properties. Initial structural analysis revealed that the pyrrolizine nucleus and the aryl-substituted structure are the major pharmacophoric features that contribute to hydrophobic and π-π interactions with the active binding sites of target proteins and play a crucial role in the overall pharmacological activity of the parent scaffold. On the other hand, the terminal carboxylate group showed relatively less involvement in the direct binding with the receptor and was considered a potential site for structural modification. Based on this rationale, a focused ligand library of amino acid-conjugated 1*H*-pyrrolizine carboxylic acid derivatives was designed by introducing structurally diverse amino acid residues including alanine, glycine, serine, proline, glutamic acid, aspartic acid, arginine and tryptophan, at the carboxylate site. This approach was expected to enhance the binding affinity, solubility, stability and other drug-like characteristics without compromising the essential pharmacophoric attributes of licofelone for subsequent computational and biological assessment.

Selection of anticancer targets: Initially, the designed compounds were docked against a diverse anticancer molecular target to identify the most relevant biological mechanisms and these targets were shortlisted based on their docking outcomes and favourable binding interactions. COX-2 and 5-LOX receptors were considered to evaluate the binding affinity of the designed analogues in comparison to their parent molecule licofelone to retain their anti-inflammatory potential by interfering COX and LOX pathways [19]. RORγ was selected to explore the antioxidant and immunomodulatory potential of the designed molecules because of its involvement in oxidative stress regulation, inflammatory signalling, immune cell differentiation and ROS-mediated cellular responses associated with cancer progression [41]. Among all screened targets, the designed molecules exhibited particularly strong binding affinity toward IDO1. IDO1 is an important immunoregulatory enzyme involved in tryptophan catabolism and its overexpression contributes for the generation of immunosuppressive tumor microenvironment to suppresses T-cell mediated immune responses for cancer progression [42]. Therefore, inhibition of IDO1 may restore antitumor immunity and represents a promising anticancer strategy. Docking analysis against COX-1 enzyme was carried out to reveal the selectivity of the designed molecules against COX enzyme to avoid any instances of side effects associated with the COX-1 inhibition.

Molecular docking: Molecular docking analysis was conducted to assess the binding affinity and molecular interaction of the designed 1*H*-pyrrolizine carboxylic acid derivatives with a panel of inflammatory and anticancer molecular targets, such as COX-1, COX-2, LOX-2, 5-LOX, IDO1 and RORγ. Molecular docking estimates the binding pose of a ligand to the active site of a receptor and allows assessment of the strength and stability of the protein-ligand interactions *via* binding energy.

The docking studies revealed that most of the designed licofelone analogues displayed similar or better binding affinities against the desired targets compared to the parent compound, suggesting successful molecular optimisation by amino acid modifications (Table-1). For COX-1, compound **8f** showed the highest binding affinity (-9.28 kcal/mol), comparable to licofelone (-9.24 kcal/mol), indicating retention of the anti-inflammatory activity. Against COX-2, compound **8e** demonstrated the strongest binding affinity (-9.89 kcal/mol), even better than licofelone (-8.99 kcal/mol) and the standard naproxen (-7.55 kcal/mol), suggesting improved target binding. Against LOX, compound **8e** showed the highest binding affinity (-7.95 kcal/ mol), followed by LSB2Phe and **8c** (-7.69 and -7.67 kcal/mol, respectively), which implies enhanced lipoxygenase inhibiting activity. For 5-LOX, the highest binding affinity was observed with LSB18Tyr (-7.38 kcal/mol), followed by the parent licofelone (-6.80 kcal/mol), suggesting that the aromatic amino acid substitution improved binding with the receptor. Interestingly, docking against indoleamine 2,3-dioxygenase 1 showed that most of the designed analogues had higher binding affinities than licofelone (-8.59 kcal/mol), with compound **8e** being the highest (-10.15 kcal/mol), followed by LSB18Tyr (-9.80 kcal/mol), **8a** (-9.37 kcal/mol) and LSP8Asp (-9.37 kcal/mol). This suggests that IDO1 could be another and possibly a more suitable anticancer target for the licofelone analogues. The docking analysis indicates that amino acid tethering at the carboxylate group of licofelone has considerably improved the binding affinity of its analogues to several therapeutic targets. Compound **8e** stood out as the most promising lead compound with strong binding

TABLE-1
BINDING ENERGY OF THE DESIGNED LICOFELONE-DERIVED PYRROLIZINE ANALOGUES AGAINST ANTICANCER TARGETS

S. No.	Compd. No.	Ligand	Binding energy (kcal/mol)					
			COX1	COX2	LOX2	5LOX	IDO1	RoRγ
			PDB: 3kk6	PDB: 5ikr	PDB: 3v99	PDB: 6n2w	PDB: 9f5r	PDB: 6q7a
1	**8a**	LSB1Ala	-7.22	-8.02	-6.95	-6.33	-9.37	-4.99
2	**8b**	LSB9Glu	-2.78	-6.43	-6.43	-5.60	-8.94	-2.23
3	**8c**	LSB17Pro	-6.09	-6.30	-7.67	-6.96	-9.16	-5.54
4	**8d**	LSB3Ser	-7.03	-8.22	-6.44	-5.93	-8.85	-5.08
5	**8e**	LSB19Trp	-4.72	-9.89	-7.95	-6.35	-10.15	-4.27
6	**8f**	LSB5Gly	-9.28	-8.86	-7.15	-6.63	-8.84	-5.74
7	**8g**	LSP8Asp	-3.27	-6.38	-6.87	-6.05	-9.37	-3.11
8	**8h**	LSB12Arg	-1.60	-5.94	-6.95	-5.12	-8.19	-1.21
9	–	LSB2Phe	-4.44	-8.98	-7.69	-6.83	-9.22	+1.41
10	–	LSB4Leu	-6.57	-6.36	-7.06	-6.84	-9.06	-1.54
11	–	LSB6Iso	-4.56	-6.02	-6.64	-6.96	-8.75	-3.68
12	–	LSB7Thr	-4.95	-5.87	-6.53	-6.85	-9.15	-3.38
13	–	LSB10Met	-5.67	-7.60	-6.01	-6.22	-9.19	-5.02
14	–	LSB11Lys	-4.16	-6.01	-6.15	-5.13	-7.67	-3.43
15	–	LSB13Cys	-3.35	-6.65	-6.69	-5.86	-8.78	-3.76
16	–	LSB16His	-3.88	-7.44	-6.54	-6.97	-8.93	-2.64
17	–	LSB18Tyr	-5.02	-6.90	-6.64	-7.38	-9.80	+0.24
18	–	Licofelone	-9.24	-8.99	-6.78	-6.80	-8.59	-9.01
19	–	Naproxen	-6.19	-7.55	-5.87	-5.43	–	-6.12
20	–	Celecoxib	-10.00	-7.42	-6.11	-5.28	–	-5.61

interactions against COX-2 and IDO1, while LSB18Tyr and **8f** also showed significant target-specific binding. These results support the development of licofelone-based amino acid conjugates as dual anti-inflammatory and immunomodulatory anticancer drug candidates.

Pharmacokinetic profiling: The detailed results for the pharmacokinetic profiling and ADMET analysis of the designed licofelone-derived pyrrolizine analogues obtained from pkCSM web server is tabulated in Table-2.

Biological evaluation

MTT assay: The antiproliferative activity of the synthesised 1*H*-pyrrolizine carboxylic acid derivatives was assessed by a 72 h MTT assay against gastric carcinoma (GSU) and pancreatic carcinoma (PANC-1) cells. The compounds were screened over the concentration range of 0.25-200 μM and the IC_{50} values are presented in Table-3. It is observed that several derivatives exhibited significantly greater cytotoxic activity than the control drugs irinotecan and 5-fluorouracil across both cell lines. In GSU cells, the most active compounds displayed IC_{50} values in the low micromolar range, particularly **8a** (4.13 ± 0.5 μM), **8d** (4.15 ± 0.9 μM), **8f** (4.1 ± 0.4 μM) and **8c** (4 ± 0.8 μM). Notably, **8b** also showed high potency (4.3 ± 0.4 μM). This was significantly lower than that of irinotecan (26.7 ± 0.23 μM) and the IC_{50} threshold of >15 μM for 5-fluorouracil in these cells. In the PANC-1 cell line, two compounds, **8c** (1.4 ± 0.05 μM) and **8b** (1.7 ± 0.2 μM), were the most active and more potent than irinotecan (9.2 ± 1 μM) and 5-fluorouracil (1.8 ± 0.03 μM). Other derivatives such as **8a**, **8d** and **8h** also displayed some activity (IC_{50} ~4-5 μM), hinting at the wide antiproliferative potential of the different structural variants. Derivatives **8c** and **8b** were identified as the most promising lead compounds for their improved antiproliferative activity.

Structure activity relationship (SAR): The SAR analysis of the designed licofelone-derived pyrrolizine analogues revealed that structural modifications with different amino acid conjugates significantly influenced their anticancer activity against gastric (GSU) and pancreatic (PANC-1) cancer cell lines. Among the synthesised analogues, **8b** and **8c** exhibited the most potent antiproliferative activity against PANC-1 cells with IC_{50} values of 1.7 ± 0.2 μM and 1.4 ± 0.05 μM, respectively, indicating that incorporation of glutamic acid and proline residues enhanced activity against pancreatic cancer cells. Comparatively, the alanine, serine and glycine substituted analogues showed moderate activity with IC_{50} values ranging 4.1-5.8 μM, suggesting that neutral unsubstituted amino acid maintained reasonable anticancer potential but cyclic or acidic amino acid conjugation results in improved anticancer potential. Interestingly, aspartic acid derivative **8g** showed significantly reduced activity against GSU cells (IC_{50} = 21 ± 2.4 μM) and only moderate activity against PANC-1 cells (IC_{50} = 10.3 ± 0.3 μM), revealing that shorter acidic side chains may adversely affect biological interactions required for anticancer effect. Most of the designed analogues exhibited superior anticancer activity compared to the standard drug irinotecan against GSU cells, while several compounds, particularly **8b** and **8c**, showed comparable or better activity than 5-fluorouracil against PANC-1 cells. Hence, the SAR findings suggest that the nature, polarity and size of amino acid substituents attached to the licofelone-derived pyrrolizine scaffold play a crucial role in modulating anticancer activity, with glutamic acid and proline substitutions emerging as the most preferred modifications for enhanced anticancer potential.

TABLE-2
PHARMACOKINETICS PROFILING AND ADMET ANALYSIS OF THE DESIGNED LICOFELONE-DERIVED PYRROLIZINE ANALOGUES

Property	Descriptor	Ideal range	**8a**	**8b**	**8c**	**8d**	**8f**	**8g**	**8h**
MW	(g/mol)	<500	450.96	509.00	477.00	466.96	436.94	509.00	536.08
LogP	–	-5 to +5	5.19	5.034	5.676	4.162	4.801	4.732	4.433
Rotatable bond	–	–	6	9	5	7	6	8	10
HBA	–	<10	3	4	3	4	3	5	4
HBD	–	<5	2	3	1	3	2	2	5
TPSA	$(Å)^2$	40-140	192.58	214.26	204.51	197.37	186.21	214.58	227.25
Absorption	Water solubility (mol/L)	–	-4.052	-2.891	-3.893	-3.111	-3.821	-4.016	-2.892
Absorption	Caco2 permeability	–	0.643	0.382	0.626	0.407	0.645	0.509	0.191
Absorption	Intestinal absorption (%) (human)	–	94.074	52.854	94.016	61.665	94.526	68.952	55.2
Absorption	Skin permeability (Log Kp)	–	-2.735	-2.735	-2.735	-2.735	-2.735	-2.735	-2.735
Absorption	P-glycoprotein substrate	–	Yes es	Yes	Yes	Yes	Yes	Yes	Yes
Absorption	P-glycoprotein I inhibitor	–	N	N	N	N	N	N	N
Absorption	P-glycoprotein II inhibitor	–	Yes	N	Yes	Yes	Yes	N	Yes
Distribution	VDss (human)	–	-0.451	-1.318	-0.344	-0.877	-0.587	-0.641	-0.022
Distribution	Fraction unbound (human)	–	0.102	0.058	0.1	0.121	0.086	0.131	0.372
Distribution	BBB permeability	–	-0.066	-1.412	0.135	-1.375	-0.102	-0.366	-1.627
Distribution	CNS permeability	–	-1.89	-2.391	-1.698	-2.382	-1.994	-2.303	-2.717
Metabolism	CYP2D6 substrate	–	Yes	Yes	Yes	Yes	Yes	N	Yes
Metabolism	CYP3A4 substrate	–	Yes	Yes	Yes	Yes	Yes	Yes	Yes
Metabolism	CYP1A2 inhibitor	–	Yes	Yes	Yes	Yes	Yes	Yes	N
Metabolism	CYP2C19 inhibitor	–	N	N	N	N	N	N	N
Metabolism	CYP2C9 inhibitor	–	Y	N	Y	Y	Y	Y	N
Metabolism	CYP2D6 inhibitor	–	N	N	N	N	N	N	N
Metabolism	CYP3A4 inhibitor	–	N	N	N	N	N	N	N
Excretion	Total clearance (log mL/min/kg)	–	0	-0.002	0.107	0.167	0.05	0.239	-0.071
Excretion	Renal OCT2 substrate	–	N	N	N	N	N	N	N
Toxicity	AMES toxicity	–	Y	N	N	N	Y	N	N
Toxicity	Max. tolerated dose (human) (log mg/kg/day)	–	0.537	0.4	0.498	0.478	0.469	0.525	0.389
Toxicity	hERG I inhibitor	–	N	N	N	N	N	N	N
Toxicity	hERG II inhibitor	–	N	N	N	N	N	N	Y
Toxicity	Oral rat acute toxicity (LD_{50}) (mol/kg)	–	2.364	2.431	2.362	2.409	2.321	2.372	2.475
Toxicity	Oral rat chronic toxicity (LOAEL) (mg/kg/day)	–	0.322	2.584	0.079	0.171	0.429	1.218	1.086
Toxicity	Hepatotoxicity	–	Y	N	Y	Y	Y	Y	Y
Toxicity	Skin Sensitisation	–	N	N	N	N	N	N	N
Toxicity	T. Pyriformis toxicity (mg/L)	–	0.285	0.285	0.285	0.285	0.285	0.285	0.285
Toxicity	MinNw toxicity	–	-1.214	-1.429	-1.3	0.186	-0.517	-4.032	4.963

TABLE-3
CYTOTOXIC ACTIVITY (IC_{50}, μM ± SD) OF 1*H*-PYRROLIZINE CARBOXYLIC ACID-AMINO ACIDS CONJUGATES AGAINST GASTRIC CARCINOMA (GSU) AND PANCREATIC CARCINOMA (PANC-1) CELLS AFTER 72 h TREATMENT

S. No.	Ligands	IC_{50} (μM ± SD)	
		GSU (gastric cancer)	PANC-1 (pancreatic cancer)
1	**8a**	4.13 ± 0.5	4.1 ± 0.5
2	**8b**	4.3 ± 0.4	1.7 ± 0.2
3	**8c**	4 ± 0.8	1.4 ± 0.05
4	**8d**	4.15 ± 0.9	4.8 ± 0.1
5	**8f**	4.1 ± 0.4	5.8 ± 1.7
6	**8g**	21 ± 2.4	10.3 ± 0.3
7	**8h**	4.83 ± 1.4	3.84 ±7
8	Irinotecan	26.7 ± 0.23	9.2 ± 1
9	5-Fluorouracil	> 15	1.8 ± 0.03

Conclusion

This work demonstrates the potential of 1*H*-pyrrolizine carboxylic acid as a promising scaffold for designing new anticancer agents targeting inflammation-driven cancer pathways. The dual inhibition of COX-2 and 5-LOX pathways offers a strategic edge in preventing tumor growth, angiogenesis and metastasis. The structural optimisation involving amino acid conjugation proved to be successful in improving the binding and interaction patterns of the designed compounds, as indicated by docking studies. The synthesised 1*H*-pyrrolizine carboxylic acid derivatives showed encouraging interaction with not only COX-2 and 5-LOX but also with novel targets in cancer therapy, such as IDO1, highlighting their potential for a multi-targeted approach. The proposed synthetic routes were effective and scalable, suggesting the potential for large scale manufacturing. In conclusion, these results suggest that

1*H*-pyrrolizine carboxylic acid derivatives have significant potential to be safer and efficient anticancer drugs. Further *in vitro* and *in vivo* studies are required to validate their biological efficacy and to explore their potential to develop novel cancer therapy.

ACKNOWLEDGEMENTS

The authors express their gratitude to the Centre of Excellence, Drug Design and Molecular Modelling at Chitkara College of Pharmacy, Chitkara University, Rajpura, India, for providing essential resources for this research.

CONFLICT OF INTEREST

The authors declare that there is no conflict of interests regarding the publication of this article.

DECLARATION OF AI-ASSISTED TECHNOLOGIES

During the preparation of this manuscript, the authors used an AI-assisted tool(s) to improve the language. The authors reviewed and edited the content and take full responsibility for the published work.

REFERENCES

1. I. Rahat, Y. Verma, K. Fatima, G. Garg and U. Farooq, *Res. Rev. Pharm. Pharm. Sci.*, **12**, (2023); https://doi.org/10.4172/2320-1215.12.4.008
2. S.M. Razavi, D. Khayatan, Z.N. Arab, S. Momtaz, K. Zare, R.M. Jafari, A.R. Dehpour and A.H. Abdolghaffari, *Prostaglandins Other Lipid Mediat.*, **157**, 106587 (2021); https://doi.org/10.1016/j.prostaglandins.2021.106587
3. F.P. Chatzipieris, E. Petsas, G. Lambrinidis, S. Vassiliou and C.T. Chasapis, *Life*, **16**, 163 (2026); https://doi.org/10.3390/life16010163
4. V. Thiruchenthooran, E. Sánchez-López and A. Gliszczyńska, *Cancers*, **15**, 475 (2023); https://doi.org/10.3390/cancers15020475
5. S. Zappavigna, A.M. Cossu, A. Grimaldi, M. Bocchetti, G.A. Ferraro, G.F. Nicoletti, R. Filosa and M. Caraglia, *Int. J. Mol. Sci.*, **21**, 2605 (2020); https://doi.org/10.3390/ijms21072605
6. P. Wang, B. Chen, Y. Huang, J. Li, D. Cao, Z. Chen, J. Li, B. Ran, J. Yang, R. Wang, Q. Wei, Q. Dong and L. Liu, *Heliyon*, **10**, e23203 (2024); https://doi.org/10.1016/j.heliyon.2023.e23203
7. S. Kulkarni and V. Pal Singh, *Curr. Top. Med. Chem.*, **7**, 251 (2007); https://doi.org/10.2174/156802607779941305
8. B. Bannwarth, *Fundam. Clin. Pharmacol.*, **18**, 125 (2004); https://doi.org/10.1046/j.1472-8206.2003.00217.x
9. G.F. Sud'ina, M.A. Pushkareva, P. Shephard and T. Klein, *Prostaglandins Leukot. Essent. Fatty Acids*, **78**, 99 (2008); https://doi.org/10.1016/j.plefa.2007.12.006
10. S. Neumann, S.A. Shirley, R.A. Kemp and S.M. Hook, *Front. Immunol.*, **7**, (2016); https://doi.org/10.3389/fimmu.2016.00537
11. W. Liu, J. Zhou, H. Zhang, H. Qian, J. Yin, K. Bensdorf and R. Gust, *Lett. Drug Des. Discov.*, **8**, 911 (2011); https://doi.org/10.2174/157018011797655223
12. R.M. Haley and H.A. von Recum, *Exp. Biol. Med.*, **244**, 433 (2019); https://doi.org/10.1177/1535370218787770
13. S. Rádl, J. Černý, O. Klecán, J. Stach, L. Plaček and Z. Mandelová, *Tetrahedron Lett.*, **49**, 5316 (2008); https://doi.org/10.1016/j.tetlet.2008.06.078
14. A. Gouda, H. Ali, W. Almalki, M. Azim, M. Abourehab and A. Abdelazeem, *Molecules*, **21**, 201 (2016); https://doi.org/10.3390/molecules21020201
15. B. Marciniak, M. Kciuk, S. Mujwar, R. Sundaraj, K. Bukowski and R. Gruszka, *Cancers*, **15**, 4442 (2023); https://doi.org/10.3390/cancers15184442
16. A. Gielecińska, M. Kciuk, E.B. Yahya, T. Ainane, S. Mujwar and R. Kontek, *Biochim. Biophys. Acta Rev. Cancer*, **1878**, 189024 (2023); https://doi.org/10.1016/j.bbcan.2023.189024
17. M. Kciuk, M. Malinowska, A. Gielecińska, R. Sundaraj, S. Mujwar, A. Zawisza and R. Kontek, *Molecules*, **28**, 7230 (2023); https://doi.org/10.3390/molecules28207230
18. Md. Kciuk, S. Mujwar, A. Szymanowska, B. Marciniak, K. Bukowski, M. Mojzych and R. Kontek, *Int. J. Mol. Sci.*, **23**, 5892 (2022); https://doi.org/10.3390/ijms23115892
19. W. Masocha, E. Aly, A. Albaloushi and A. Al-Romaiyan, *Biomedicines*, **12**, 1545 (2024); https://doi.org/10.3390/biomedicines12071545
20. F.P. Chatzipieris, E. Petsas, G. Lambrinidis, S. Vassiliou and C.T. Chasapis, *Life*, **16**, 163 (2026); https://doi.org/10.3390/life16010163
21. C. Chang, S. Ekins, P. Bahadduri and P.W. Swaan, *Adv. Drug Deliv. Rev.*, **58**, 1431 (2006); https://doi.org/10.1016/j.addr.2006.09.006
22. G. Klebe, Pharmacophore Hypotheses and Molecular Comparisons, In: Drug Design. Springer Berlin Heidelberg; pp. 349-370 (2013); https://doi.org/10.1007/978-3-642-17907-5_17
23. A.A. Bhat, M. Ahmed, N. Elboughdiri, P. Thakur, V. Natarajan, A.F. El-kott, B.S. Rajab, S. Alghamdi, J. Singh, A.K. Wani and A. Hameed, *Drug Dev. Res.*, **87**, e70262 (2026); https://doi.org/10.1002/ddr.70262
24. H. Wang, Q. Yao, Y. Guo, Q. Zhang, Z. Wang, R.J. Strasser, S. Chen, B.E. Valverde, S. Qiang and H.M. Kalaji, *J. Adv. Res.*, **40**, 29 (2022); https://doi.org/10.1016/j.jare.2021.12.001
25. S. Bhatt, B. Patel, A. Patel, S. Daftari, H. Bhatt, S.K. Dalai and V.K. Vyas, *Lett. Drug Des. Discov.*, **23**, 100371 (2026); https://doi.org/10.1016/j.lddd.2026.100371
26. K.R. Cousins, *J. Am. Chem. Soc.*, **127**, 4115 (2005); https://doi.org/10.1021/ja0410237
27. M. Kciuk, N. Garg, S. Dhankhar, M. Saini, S. Mujwar, S. Devi, S. Chauhan, T.G. Singh, R. Singh, B. Marciniak, A. Gielecińska and R. Kontek, *Pharmaceuticals*, **17**, 701 (2024); https://doi.org/10.3390/ph17060701
28. P.J. Chaudhari, S.B. Bari, S.J. Surana, A.A. Shirkhedkar, C.G. Bonde, S.C. Khadse, V.G. Ugale, A.A. Nagar and R.S. Cheke, *ACS Omega*, **7**, 17270 (2022); https://doi.org/10.1021/acsomega.2c01198
29. M. Kciuk, A. Gielecińska, S. Mujwar, M. Mojzych and R. Kontek, *Biochim. Biophys. Acta Rev. Cancer*, **1877**, 188716 (2022); https://doi.org/10.1016/j.bbcan.2022.188716
30. H.M. Berman, J. Westbrook, Z. Feng, G. Gilliland, T.N. Bhat, H. Weissig, I.N. Shindyalov and P.E. Bourne, *Nucleic Acids Res.*, **28**, 235 (2000); https://doi.org/10.1093/nar/28.1.235
31. H.M. Berman, T. Battistuz, T.N. Bhat, W.F. Bluhm, P.E. Bourne, K. Burkhardt, Z. Feng, G.L. Gilliland, L. Iype, S. Jain, P. Fagan, J. Marvin, D. Padilla, V. Ravichandran, B. Schneider, N. Thanki, H. Weissig, J.D. Westbrook and C. Zardecki, *Acta Crystallogr. D Biol. Crystallogr.*, **58(6I)**, 899 (2002); https://doi.org/10.1107/S0907444902003451
32. G.M. Morris, R. Huey, W. Lindstrom, M.F. Sanner, R.K. Belew, D.S. Goodsell and A.J. Olson, *J. Comput. Chem.*, **30**, 2785 (2009); https://doi.org/10.1002/jcc.21256
33. S. Forli, R. Huey, M.E. Pique, M.F. Sanner, D.S. Goodsell and A.J. Olson, *Nat. Protoc.*, **11**, 905 (2016); https://doi.org/10.1038/nprot.2016.051
34. BIOVIA, Dassault Systèmes, [Biovia Discovery Studio], San Diego: Dassault Systèmes (2024).
35. N. Agrawal, S. Mujwar, A. Goyal and J.K. Gupta, *Lett. Drug Des. Discov.*, **19**, 69 (2022); https://doi.org/10.2174/1570180818666210813121431

36. P. Pradhan, N.K. Soni, L. Chaudhary, S. Mujwar and K.R. Pardasani, *Biosci. Biotechnol. Res. Asia*, **12**, 2173 (2015); https://doi.org/10.13005/bbra/1889
37. D. Iqbal, M. Alsaweed, Q.M.S. Jamal, M.R. Asad, S.M.D. Rizvi, M.R. Rizvi, H.M. Albadrani, M. Hamed, S. Jahan and H. Alyenbaawi, *Biomolecules*, **13**, 1613 (2023); https://doi.org/10.3390/biom13111613
38. M. Mohanty and P.S. Mohanty, *Monatsh. Chem.*, 157, 683 (2023); https://doi.org/10.1007/s00706-023-03076-1
39. P.N. Sonwane and M.R. Kumbhare, *Sci. Rep.*, **15**, 35270 (2025); https://doi.org/10.1038/s41598-025-18084-w
40. A. Mathakiya, B. Patel, K. Raval, J.H. Kamdar, S. Sharma and J. Dhalani, *Results Chem.*, **16**, 102521 (2025); https://doi.org/10.1016/j.rechem.2025.102521
41. J. Li, C. Huang, P. Tang, R. Wu, Q. Wu and C. Zhang, *J. Hematol. Oncol.*, **19**, 16 (2026); https://doi.org/10.1186/s13045-026-01780-z
42. L. Zhai, A. Bell, E. Ladomersky, K.L. Lauing, L. Bollu, J.A. Sosman, B. Zhang, J.D. Wu, S.D. Miller, J.J. Meeks, R.V. Lukas, E. Wyatt, L. Doglio, G.E. Schiltz, R.H. McCusker and D.A. Wainwright, *Front. Immunol.*, **11**, 1185 (2020); https://doi.org/10.3389/fimmu.2020.01185